Impact of land use change on regional carbon sink capacity: Evidence from Sanmenxia, China

Ecological Indicators 156 (2023) 111189

Contents lists available at ScienceDirect

Ecological Indicators

journal homepage: www.elsevier.com/locate/ecolind

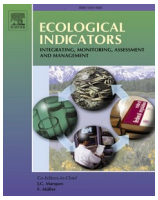

Impact of land use change on regional carbon sink capacity: Evidence from Sanmenxia, China

Yisha Pan [a], Hebing Zhang [a,*], Chongyang Wang [b], Yongduo Zhou [a]

[a] School of Surveying and Land Information Engineering, Henan Polytechnic University, Jiaozuo, Henan 454000, China
[b] School of Resources and Safety Engineering, Chongqing University, Chongqing 400044, China

ARTICLE INFO

Keywords:
Carbon sequestration capacity
Land utilization
FLUS model

ABSTRACT

Regional carbon sink fluctuations are largely influenced by land use. To enhance regional carbon sink and inform sustainable land management practices, it is critical to elucidate the influence of land use changes on carbon sink dynamics. Employing historical data on carbon sink in Sanmenxia region, this study analyzed alterations in land use and carbon sink between 2000 and 2020. The Future Land Use Simulation (FLUS) model was used to predict the impacts of land use type changes on regional carbon sink under three development scenarios (urban priority, cultivated land priority, and ecological priority).The result shows that:(1) From 2000 to 2020, cultivated land (with an increase of 3.26%) and construction land (with an increase of 22.85%) showed the most significant changes, with the main source of increase being grassland, while other land types showed little change. The southern part of the study area was mainly forest land and grassland, with higher carbon sink value than the northern part. (2) The simulation study of the three scenarios found that the development scenarios of ecological priority and cultivated land priority would be conducive to improving regional carbon sink value by 2040. Specifically, regional cropland, forest, and grassland were preserved due to the ecological red line and the restriction of basic farmland. This would increase the carbon sink value of the study area by 145 thousand tons and 171 thousand tons, respectively, compared with 2020. (3) The prediction results of the three development scenarios all showed that the carbon sink of the study area would decline first and then increase from 2020 to 2040. The carbon sink of the urban priority scenario would reach the lowest value in 2030, and the other development scenarios would reach the lowest value around 2028, and then increase significantly.

1. Introduction

Land use change is one of the main drivers of carbon cycling in terrestrial ecosystems. Initially, vegetation photosynthesis and respiration exchange CO_2 and O_2 with the atmosphere, influencing regional carbon sink changes. Moreover, different land use types considerably impact soil carbon sinks (Wang et al., 2021a). These changes will eventually affect regional carbon cycle, and carbon sequestration has become a hot topic recently (Rhys et al., 2021; Michael et al., 2020; Díaz-Puente et al., 2021).

Over 30 % of carbon emissions caused by human activities originate from land use changes (Yi et al., 2022). By simulating the land use patterns in various scenarios, the changes of carbon sink caused by different land use patterns could be further calculated (He et al., 2023). To mitigate global warming, land space planning must focus on low-carbon optimization and carbon sink enhancement. Various models, including the CA-Markov coupling model (Lin et al., 2021), Logistic-CA, InVEST, and others (Zhao et al., 2023; Zhang et al., 2021; Nel et al., 2022), have been used by many researchers to simulate regional land use. As research deepens and neural networks evolve, Liu et al. (2017) established the FLUS coupling model, which demonstrates high simulation accuracy (Zhu et al., 2017; Li et al., 2023).

With the ongoing advancements in land use driving mechanisms, urban planning, policy formulation, and land use evaluation research, modeling and simulation of land use have emerged as critical tools. These tools are used to explore the significant impacts of land use changes on the ecological environment. Alison et al. (2016) argued that environmental alterations and carbon storage shifts due to land use modifications bear significant implications for future land use decision-making. By investigating the influence of forest carbon sinks on Australia's climate, Josephine (2023) suggested that enhancing forest carbon sinks aids in conforming to Australia's carbon emission objectives

* Corresponding author.
E-mail address: zhbhpu@163.com (H. Zhang).

https://doi.org/10.1016/j.ecolind.2023.111189
Received 17 August 2023; Received in revised form 26 October 2023; Accepted 29 October 2023
Available online 1 November 2023

and adapting to climate change.

Numerous studies have delved into the evolution of carbon sinks in relation to land use spatial configurations and the underlying drivers. Letourneau et al. (2012) proposed a novel approach to classify and model land use, employing a Land Use System-based (LUS) method. This considers factors such as population density, market accessibility, land use/cover categorization, and livestock concentration. Barati et al. (2022) studied the interaction between LUCC and climate change during the 50-year period from 1966 to 2015, and the results showed that the direct effect of pasture use change was positive, and its indirect effect was negative. In addition, deforestation increases CO_2 emissions indirectly. Noting that LUCC can alter the ability of ecosystems to provide services to humans, it is critical to identify the patterns, trends, and impacts of climate change. Projects such as grain for green (grass) and ecological restoration can significantly enhance regional carbon sink capacity (An et al., 2019; Ma and Wang, 2015) Embracing sustainable development concepts, Sanmenxia has strenuously pursued wetland conservation, mine restoration, and forest land expansion to enhance the carbon sink effect of land use (Xu et al., 2023).

Irrational land use can negatively impact the ecological environment and impede socio-economic development (Wang et al., 2023a). Paying heed to the carbon sink functionality of grassland, wetland, and natural forest land, while reasonably adjusting the proportion of cultivated and construction land under "cultivated land red line" restrictions, constitutes a critical approach to augmenting regional carbon sequestration and increasing carbon sink (Huang et al., 2023; Rao et al., 2021).

Currently, literature on the prediction of future carbon sink trajectories is sparse. By simulating the land use conditions in the study area under three different scenarios, we quantified and analyzed the spatial–temporal changes of carbon sink in the study area, which could provide scientific reference for future urban land use management, low-carbon green development and regional ecological protection.

The study area belongs to the hilly and mountainous region of western Henan, with various land use types and certain representativeness. With the rapid development of social economy, the spatial pattern of land use in the study area has changed greatly. There was a lack of studies on the temporal and spatial dynamics of carbon sink in the study area. Our research delved into the interrelation between land use and carbon sink, elucidating the spatio-temporal metamorphosis and distributional characteristics of carbon sink in the vicinity. We pioneeringly projected the carbon sink alteration traits and pinpointed the moment of carbon peak in the study area under the lens of three varied development paradigms. Such insights pave the way for informed ecological preservation and low-carbon land utilization strategies in the region.

2. Study area overview

Sanmenxia, situated at the intersection of Henan, Shanxi, and Shaanxi provinces in western Henan Province, spans a total area of 10,496 square kilometers. The city's geographical location ranges from 33°31′24″N to 35°05′48″N and from 110°21′42″E to 112°01′24″E. The region features a warm temperate continental monsoon semi-arid climate. Sanmenxia's topography is diverse (see Fig. 1), predominantly comprising mountains (54.8 % of the total area), hills (36 %), and loess tablelands (9.2 %). The city hosts many rivers that flow into the Yellow River and the Yangtze River. The modifications in land use types and vegetation structure greatly impact the carbon sink capacity in the study area. Recent projects such as wetland restoration, mine ecological restoration, and urban green corridor construction have fostered Sanmenxia's green development, enhancing regional carbon sink capacity and prompting adjustments in land use structure.

3. Data sources and research methods

3.1. Data sources

The FLUS model requires data on land use, natural factors, social factors, and limiting factors. This study employs five periods of land use raster data (2000, 2005, 2010, 2015, and 2020) from Sanmenxia, sourced from the Resources and Environmental Science and Data Center of the Chinese Academy of Sciences. The spatial resolution is 30 m. Based on its topographic and geomorphic characteristics, the DEM (from geospatial data cloud website, spatial resolution: 30 m), slope (calculated from DEM), distance from the water area (obtained by the Euclidean distance based on data from Sanmenxia Natural Resources and Planning Bureau), annual average rainfall and annual average temperature (National Earth System Science Data Center (https://loess.geodata.cn), 1 km resolution) were taken as natural factors affecting regional spatial development. In terms of social factors, the spatial resolution of the rasted-data of GDP and population (from the Center for Resources and Environmental Science and Data (https://www.resdc.

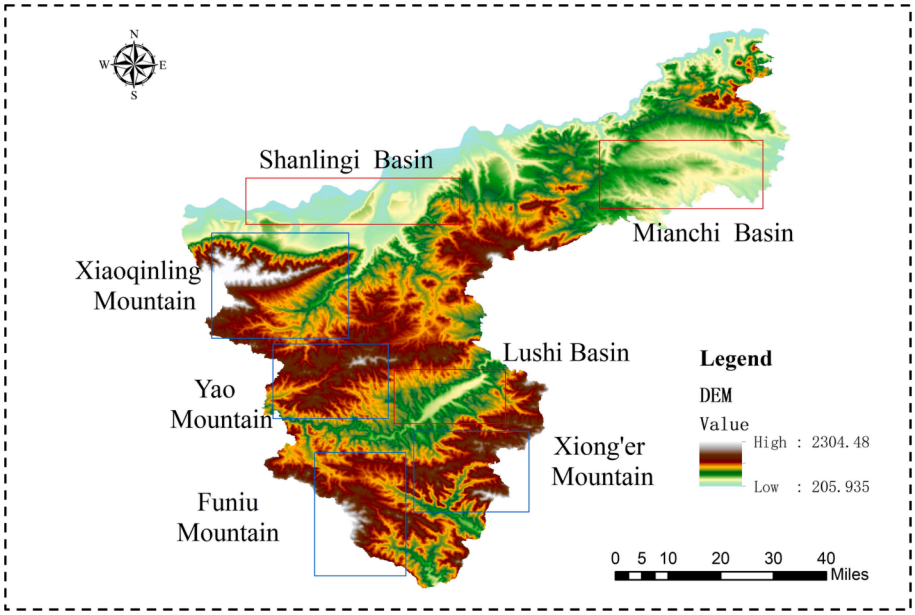

Fig. 1. Topographic map of Sanmenxia.

cn)) was unified, and the Euclidean distance was calculated for the data of railway and road (from the same source as the distance from water). The limiting factors, encompassing urban development boundaries, permanent basic farmland, and ecological protection red lines, were obtained from Sanmenxia Natural Resources and Planning Bureau.

3.2. Research methods

3.2.1. Data processing

The land use data of Sanmenxia from 2000 to 2020 was reclassified into six categories in accordance with the Land-Use and Land-Cover Change (LUCC) system: cultivated land, forest land, grassland, water area, construction land, and unused land. Natural factors, social factors, and limiting factors were cropped and resampled to unify their coordinates and spatial resolution. The change of land use type in the study area was evaluated through the land use transition matrix. The carbon sinks of various land uses were calculated via the carbon density method, facilitating the analysis of the temporal and spatial evolution of the carbon sink.

3.2.2. FLUS model

Future land use simulation model (FLUS) is a prediction model that combines an enhanced cellular automata model with a multilayer feedforward neural network algorithm to study land use and land cover scenarios under the impact of natural and human activities (Wang et al., 2020). The GeoSOS-FLUS model extracts and defines interaction rules from training data, simulates, and optimizes by obtaining initial conditions combined with interaction rules (He et al., 2020; Robinson et al., 2018). It further optimizes and updates the state and environment through iteration, finally coupling simulation with optimization (see Fig. 2). The Markov model was initially used to gain the probability matrix between land use types in the two periods and to forecast the land demand structure in 2035 under the natural development scenario (Li et al., 2020). Next, the conversion probabilities of different land use types were calculated using neural network cellular automata (CA) coupled with driving force factors. The adaptive inertia competition mechanism based on roulette can address the complexity and uncertainty of land use change and achieve the simulation results. Lastly, by setting different land use conversion matrices and neighborhood factor parameters, the land use pattern of Sanmenxia in 2035 under three scenarios of urban, cultivated land, and ecological priority was simulated and predicted.

(1) Artificial neural networks are typically composed of an input layer, a hidden layer, and an output layer. They can be expressed with the following formula:

$$p(k,t,l) = \sum_j w_{j,k} \times sigmoid\left[net_j(k,t)\right]$$

$$= \sum_j w_{j,k} \times \frac{1}{1+e^{net_j(k,t)}} \quad (1)$$

where: $p(k,t,l)$ represents the suitability probability of transformation for the first l land use type in unit k and at time t; $w_{j,k}$ denotes the input layer and hidden layer, the parameters (weights) between $net_j(k,t)$ are the signal received by the jth neuron in the hidden layer in unit k and at time t; and *sigmoid* is an activation function of hidden layers.

Introducing a random item $RA = 1 + (-ln\gamma)^{\alpha}$, where γ is a random number between 0 and 1, and α is a parameter controlling the size of a random variable, we can modify Equation (1) into:

$$p(k,t,l) = RA \times \sum_j w_{j,k} \times \frac{1}{1+e^{net_j(k,t)}}$$

$$= (1+(-ln\gamma)^{\alpha}) \times \sum_j w_{j,k} \times \frac{1}{1+e^{net_j(k,t)}} \quad (2)$$

In training samples for neural networks, the input layer (data of driving factors) generally undergoes standardization to constrain the input value within the range of 0 to 1. The training method utilized random sampling, and the sample quantity varied with the proportion of different classes. Setting the number of hidden layers to 13, we obtained the suitability probability for various land uses in the study area through iterative cycling.

(2) The weight of the neighborhood influence factor in the cellular automata (CA) model as proposed by Yu et al. (2023) reflecting the interaction between units of different land use types within the neighborhood, is expressed by the following formula:

$$\Omega_{p,k}^{t} = \frac{\sum_{N\times N} con\left(C_p^{t-1} = k\right)}{N \times N - 1} \times W_k \quad (3)$$

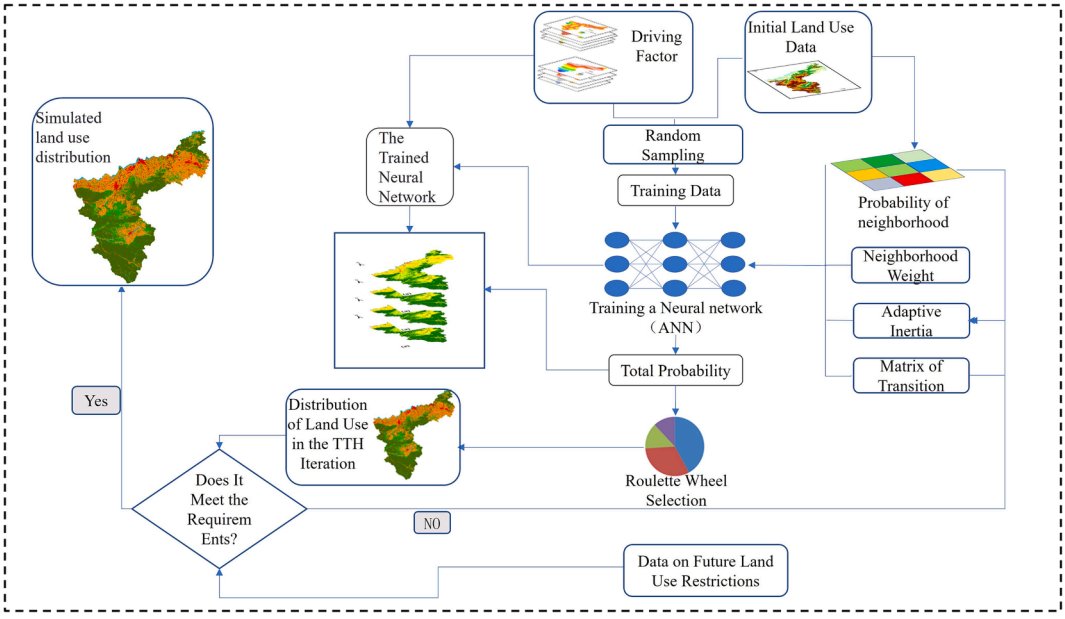

Fig. 2. Framework of the FLUS model.

where $\Omega_{p,k}^{t}$ represents the neighborhood effect of the land use type k on raster p at time t, $\sum_{N\times N} con\left(C_p^{t-1}=k\right)$ said in the N × N field of Moore denotes the total number of grids for the kth land type at time t, and W_k is a function of various land use type neighborhood and weights of the range between 0 and 1.

(3) An adaptive inertia coefficient allows the inertia coefficient to adjust according to the gap between the current scale and target scale of a specific land use type. The adaptive inertia coefficient of the kth land type at time t is:

$$Inertia_k^t=\begin{cases} Inertia_k^{t-1}\left(\left|D_k^{t-2}\right|\le\left|D_k^{t-1}\right|\right) \\ Inertia_k^{t-1}\times\dfrac{D_K^{t-2}}{D_k^{t-1}}\left(0\ge\left|D_k^{t-2}\right|\ge\left|D_k^{t-1}\right|\right) \\ Inertia_k^{t-1}\times\dfrac{D_K^{t-1}}{D_k^{t-2}}\left(\left|D_k^{t-1}\right|>\left|D_k^{t-2}\right|>0\right) \end{cases} \tag{4}$$

where D_K^{t-1} and D_K^{t-2} are respectively the difference between the number of grids of the kth land type and the demand quantity at time t-1 and t-2.

In summary, the comprehensive probability calculation formula is expressed as follows:

$$Tp(k,t,l)=RA\times p(k,t,l)\times\Omega_{p,k}^{t}\times Inertia_k^t \tag{5}$$

3.3. Carbon sink calculation

The carbon density method calculates both vegetation and soil carbon sinks (Yang et al., 2017). For vegetation carbon sinks, the biomass of cultivated land, forest land, and grassland was taken into account, and the carbon density method was used. The corresponding calculation formula is:

$$Q=A\times d_1+B\times d_2+C\times d_3 \tag{6}$$

where Q symbolizes the total vegetation carbon sink, t; A, B, and C denote the areas of cultivated land, forest land, and grassland in the study area (hm^2), respectively; d_1, d_2, and d_3 are the carbon densities of cultivated land, forest land, and grassland, t/hm^2, respectively.

Regarding soil carbon sinks, the soil constitutes one of the most extensive carbon pools in terrestrial ecosystems, containing numerous carbon sink resources.

Based on the results of prior research and the average soil carbon density of different land use types in the study area, the soil carbon density method was selected to measure the soil carbon sink (Zhang et al., 2013). The calculation formula is:

$$C_S=\sum_{i=1}^{n}(H_iM_i) \tag{7}$$

where C_S signifies the total soil carbon sequestration, t; H_i denotes the area of each land type, hm^2; and M_i is the soil organic carbon density corresponding to the area of each land type, t/hm^2.

To accurately estimate the carbon sink within our study area, we must account for the vegetation and soil carbon densities linked to each land type in the region. The carbon densities of soils and vegetation vary substantially across diverse areas. Considering China's soil census data and relevant research specific to this region (Zhang et al., 2013), the following carbon densities have been selected for soil and vegetation (see Table 1):

4. Analysis of research results

4.1. Area changes of land use types

Table 2 highlights that the primary land use types in Sanmenxia are cultivated land, forest land, and grassland. Combined, these account for 94 % of the city's total area. Conversely, the areas designated as water, construction land, and unused land are minimal, comprising roughly 6 % of the total city area. Between 2000 and 2020, Sanmenxia's land-use structure experienced minimal changes. The land use categories encompassed forest land, cultivated land, grassland, construction land, water area, and unused land. Over the 20-year period, increases were recorded for cultivated land (by 10523.9 hm^2), forest land (by 4274.3 hm^2), construction land (by 10330.58 hm^2), and unused land (by 26.05 hm^2). However, grassland and water area experienced decreases of 24893.9 hm^2 and 322.11 hm^2, respectively.

The land-use transfer matrix showed that changes mainly occurred among grassland, construction land, cultivated land, and forest land. Notably, 65 % of the reduced grassland area was converted into cultivated land, while 33 % was transformed into construction land and forest land. The predominant sources of increased cultivated land included grassland (58 %), forest land (21 %), construction land (12 %), and water area (8 %). In contrast, increases in construction land primarily arose from cultivated land (79 %), grassland (12 %), and forest land (6 %).

Fig. 3 presents the spatial distribution map of land use for 2000 and 2020. It demonstrates a consistent trend of cultivated land in Sanmenxia eroding grassland, leading to a significant reduction in grassland area. Construction land has significantly expanded, while the forest area has remained relatively stable. Localized enlargements were selected from areas A (Lingbao City), B (Shanzhou District, Binhu District), C (Mianchi County, Yima City), and D (Lushi County).

In 2020, comparing the three regions B, C, and D shows denser red spots on the land class map than in 2000, indicating a more apparent expansion of construction land. Region A's comparison reveals an expansion of cultivated land and significant reduction in grassland area by 2020. As the socioeconomic development and urbanization of Sanmenxia's counties and cities progress, the demand for construction land escalates. Consequently, the areas of urban construction land in the four regions have significantly increased in 2020 compared to 2000.

Table 1
Carbon densities of soil and vegetation in Sanmenxia.

Type of land use	Cultivated land	Forest land	Grassland	Construction land	Unused land
Vegetation carbon density (t/hm^2)	12.2	20.8	15.1	–	–
Soil carbon density (t/hm^2)	91	99.4	92	86.8	81.5

Table 2
Carbon sinks in Sanmenxia from 2000 to 2020.

	2000	2005	2010	2015	2020	Rate of carbon sink change in 20 years
Cultivated land	33.20	33.34	34.91	34.51	34.28	0.03
Forest land	50.78	50.72	51.15	51.17	51.29	0.01
Grassland	20.04	20.00	17.66	17.63	17.37	−0.13
Construction land	3.72	3.80	4.14	4.37	4.57	0.23
Unused land	0.03	0.04	0.01	0.01	0.03	0.07
Soil carbon sink	92.19	92.32	92.36	92.26	92.17	−0.0002
Vegetation carbon sink	15.54	15.54	15.47	15.42	15.38	0.01
Aggregate	107.73	107.85	107.83	107.68	107.55	−0.002

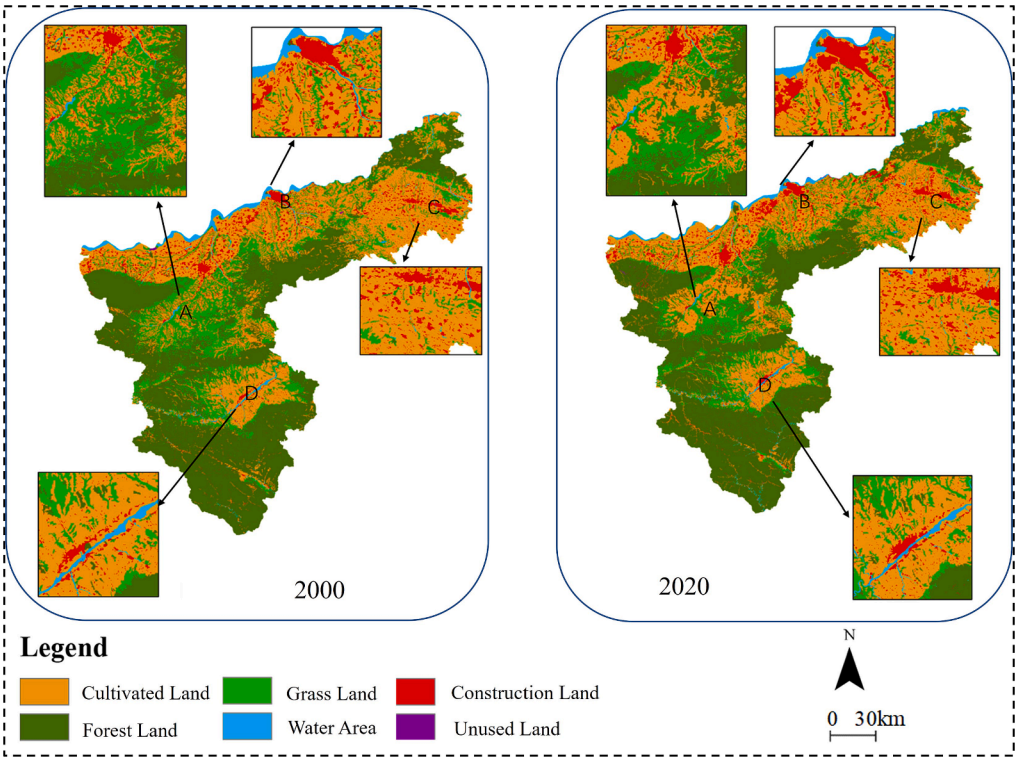

Fig. 3. Spatial distribution map of land use for 2000 and 2020.

4.2. Changes in carbon sink of land use

Given the changes in Sanmenxia's land use, we calculated the carbon sink for various land types using the carbon density method. The carbon sink for each land use period was computed from 2000 to 2020, and the changes were summarized in Table 3.

Table 3 demonstrates that, from 2000 to 2020, Sanmenxia's land use carbon sink follows a trend of initial increase followed by a decrease. Over 85 % of the total carbon sink was attributable to the soil carbon sink. Among the changes in different types of carbon sinks, grassland's carbon sink decreased from 20.03 million tons in 2000 to 17.37 million tons in 2020, showing a 13 % reduction over the 20-year span. The carbon sinks of cultivated land, forest land, and unused land experienced some fluctuations, while the carbon sink of construction land displayed a consistent increase—from 3.72 million tons in 2000 to 4.57 million tons in 2020, signifying a 23 % increase.

The carbon sink for land use in Sanmenxia is visualized via zoning on a map at the township unit level (see Fig. 4. Notably, the regional carbon sink presents clear regional differences. Fig. 4 indicates that Lushi County, located in the southern part of Sanmenxia, maintains a higher carbon sink. Conversely, Lingbao City, Shanzhou District, and Binhu District in the north, along with Mianchi County and Yima City in the east, register a lower carbon sink due to their relatively concentrated urban areas.

Table 3
Carbon sink of Sanmenxia from 2000 to 2020 (million tons).

	2000	2005	2010	2015	2020	Rate of change over 20 years
Cultivated land	33.20	33.34	34.91	34.51	34.28	0.03
Forest land	50.78	50.72	51.15	51.17	51.29	0.01
Grassland	20.04	20.00	17.66	17.63	17.37	−0.13
Water area	3.72	3.80	4.14	4.37	4.57	0.23
Construction land	0.03	0.04	0.01	0.01	0.03	0.07
Soil carbon sink	92.19	92.32	92.36	92.26	92.17	−0.0002
Vegetation carbon sink	15.54	15.54	15.47	15.42	15.38	0.01
Total	107.73	107.85	107.83	107.68	107.55	−0.002

Note: Kindly check credit author text.

The carbon sink for land use in Lushi County remained stable from 2000 to 2020 with minimal changes. Around the primary urban areas in Lingbao City, Mianchi County, and Yima City, the average growth of the carbon sink was notable. Conversely, due to the expansion of urban development and construction land, the average carbon sink value in Binhu District, Shanzhou District, and Mianchi County showed a downward trend.

By comparing the carbon sinks of each township in Sanmenxia from 2000 to 2020, a spatial distribution of carbon sink changes over the past 20 years can be mapped. According to the rate of change (R) Sanmenxia were categorized into five levels: significantly decreased ($-3.7 \leq R < -1$), decreased($-1 \leq R < -0.15$), stable($-0.15 \leq R < 0.1$), increased($0.1 \leq R < 0.15$), and significantly increased($0.15 \leq R < 0.19$). As shown in Fig. 5, the carbon sink in most areas of Sanmenxia underwent minor changes over the 20-year span. However, the carbon sink in Wumiao Township, Sucun Township, Xiyan Township, Dawang Town, and several streets in Mianchi County increased significantly. In contrast, the carbon sink in the main urban area and Nancun Township of Sanmenxia counties and cities decreased notably, with the most substantial reductions occurring in Lingbao City and Mianchi County.

4.3. Prediction results of the FLUS model

4.3.1. Land use prediction results

The Markov model was employed with 2000 as the initial year to predict the demand area for various land uses in 2020. This prediction was compared to the actual land use areas in 2020. The comparative results are shown in Fig. 6. It can be inferred from the figure that the

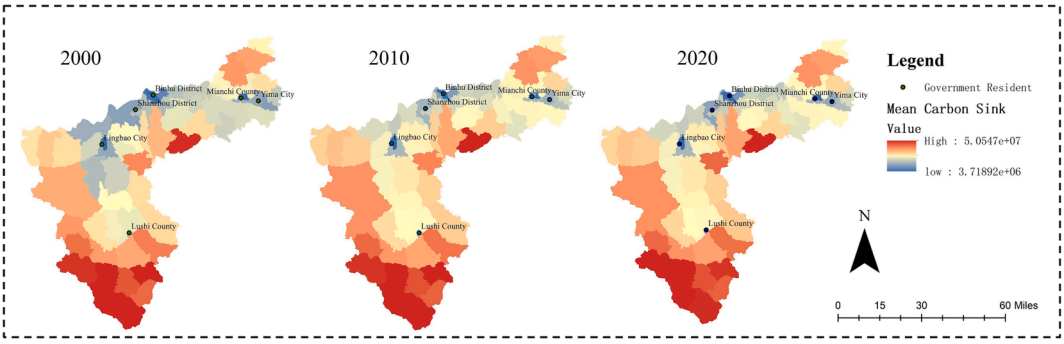

Fig. 4. Distribution map of land use carbon sink in Sanmenxia.

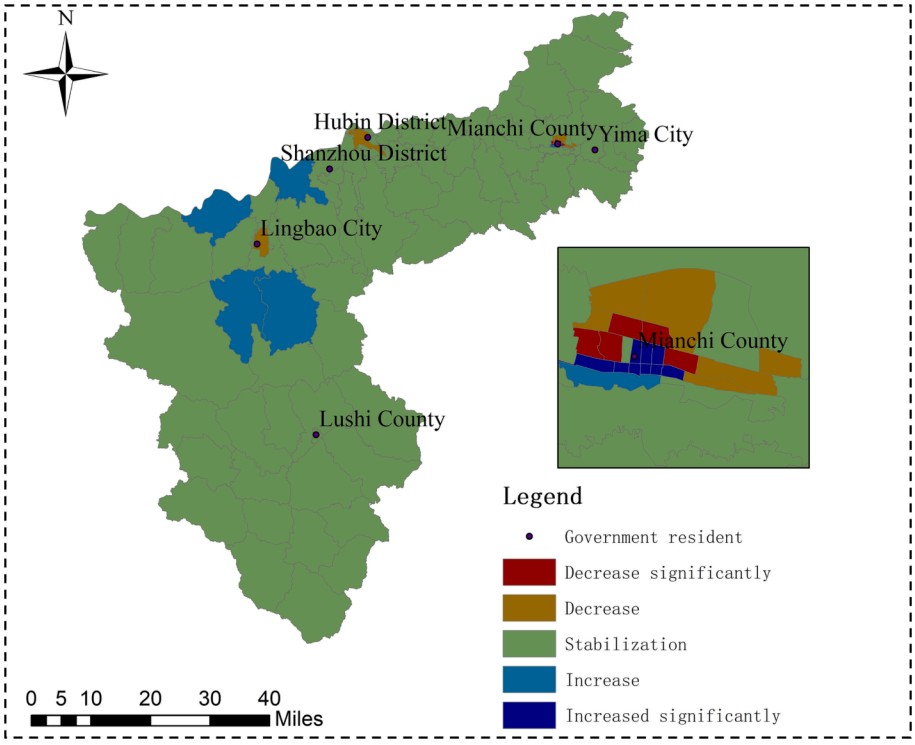

Fig. 5. Distribution of carbon sink changes in Sanmenxia.

discrepancy between the actual area and the simulated area in 2020 is minimal, and the error across various types of land use ranges from −0.3 to 0.1. This indicates that the model's simulation accuracy fulfills the research requirements.

Land use data, driving factors, urban development boundaries, permanent basic farmland, ecological protection red lines from 2000, and predictions of different land types' areas in 2020 based on the Markov model were fed into the FLUS model. Testing was then performed on the actual land use area within the study region in 2020. A calculated Kappa coefficient of 83 % demonstrated high accuracy in the simulation results.

For the future land use status prediction of Sanmenxia under different scenarios, the 2020 land use data from the city were set as the starting point. Relevant data for the city were then incorporated into the FLUS model. Simulations and predictions were made by configuring relevant limiting development factors under three development scenarios—urban priority, cultivated land priority, and ecological priority. Iterative operation of the model allowed the prediction of Sanmenxia's land use in 2040 under these different scenarios. Simulation results are displayed in Fig. 7. Land use simulation within the study area was influenced by different limiting factors, and the land space development situation largely conformed to the three development scenarios. Overall, land use under the ecological priority development scenario showed comparative advantages.

To more clearly identify changes in land types, two typical areas—Lingbao City (A) and the combined area of Mianchi County and Yima City (D)—were selected for localized magnification, as shown in Fig. 7. Compared to the three development scenarios, construction land areas in the two regions under the urban priority scenario were more concentrated. The extent of construction land in the main urban area was large, expanding towards the outskirts and noticeably transforming grassland and cultivated land into construction land. Under both cultivated land priority and ecological priority scenarios, the central urban area construction land area was smaller, and peripheral construction land was more scattered and smaller compared to the urban priority scenario. Cultivated land was preserved, grassland area was significantly larger than in the urban priority scenario, and ecological carbon sink compensation occurred.

4.3.2. *Prediction results of the land use carbon sink*

The FLUS model was used to predict the 2040 land use status of Sanmenxia under urban priority, cultivated land priority, and ecological

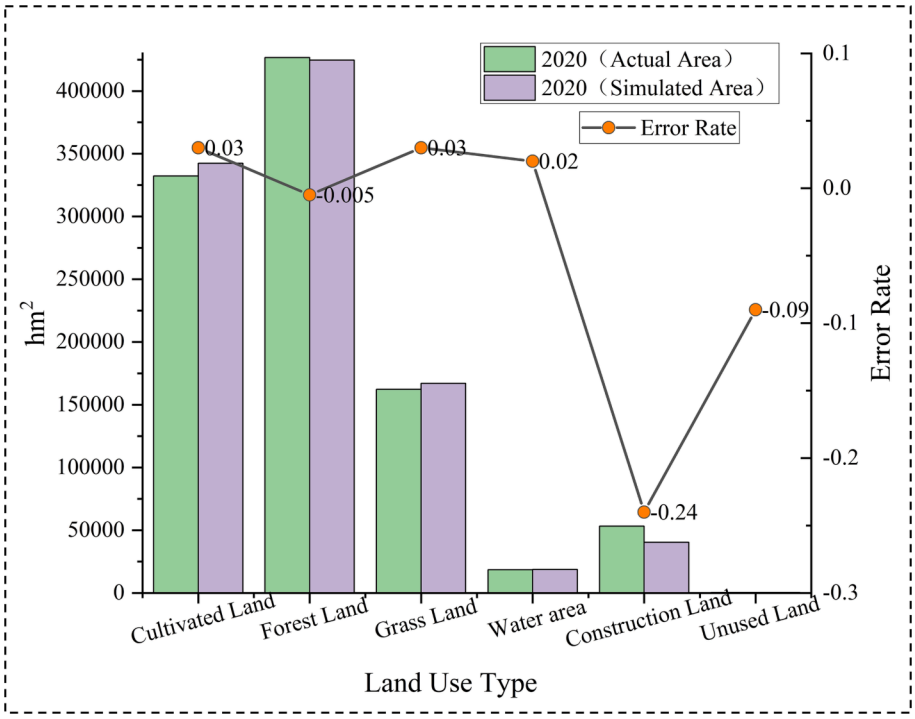

Fig. 6. Comparison and error between actual area and simulated area in 2020.

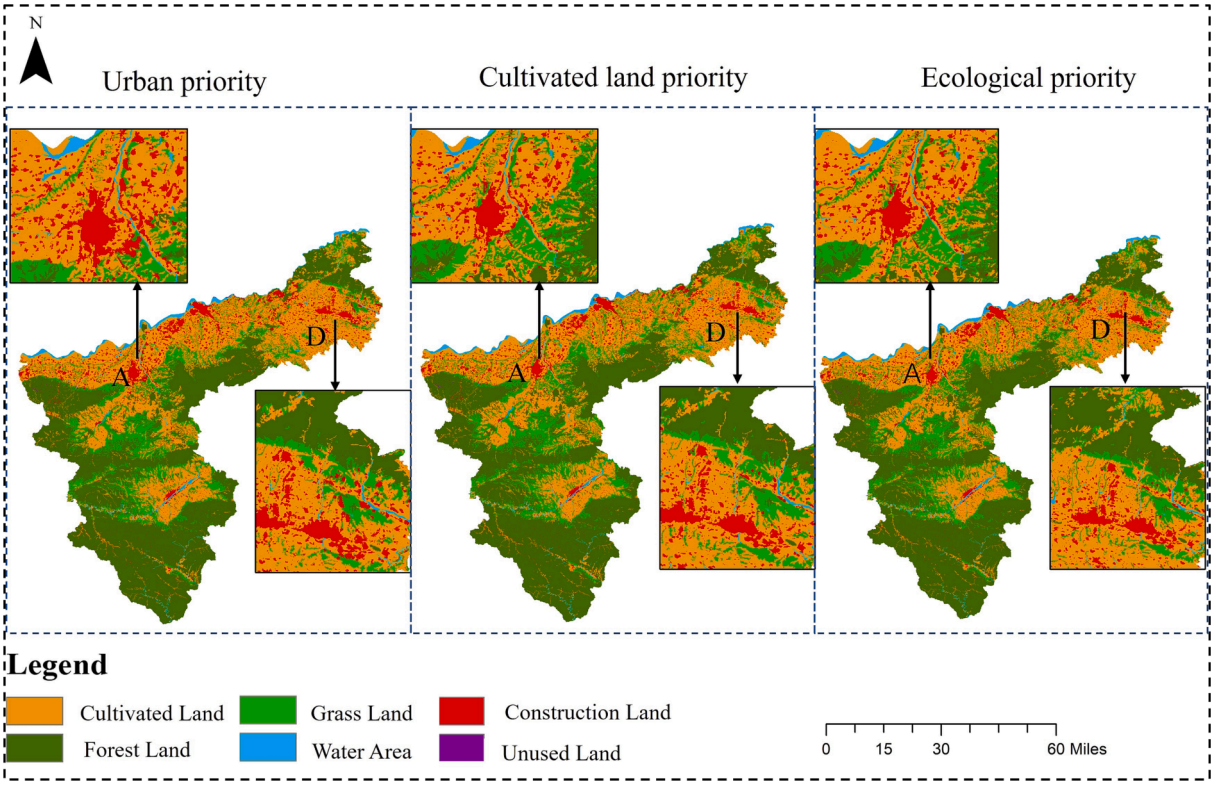

Fig. 7. Land use simulation results in 2040.

priority scenarios, as illustrated in Fig. 8. In the urban priority development scenario, the urban development boundary served as the limiting factor. Predictions showed an increase in the areas of cultivated land, forest land, and construction land in Sanmenxia in 2040 compared to 2020. Notably, the construction land area experienced the greatest increase at 11 %, while the areas of grassland, water, and unused land decreased, with unused land area reducing by 14 %.

Under the cultivated land priority development scenario, the inclusion of Sanmenxia's basic farmland data as a limiting factor led to predictions that cultivated land and forest land would still increase, while

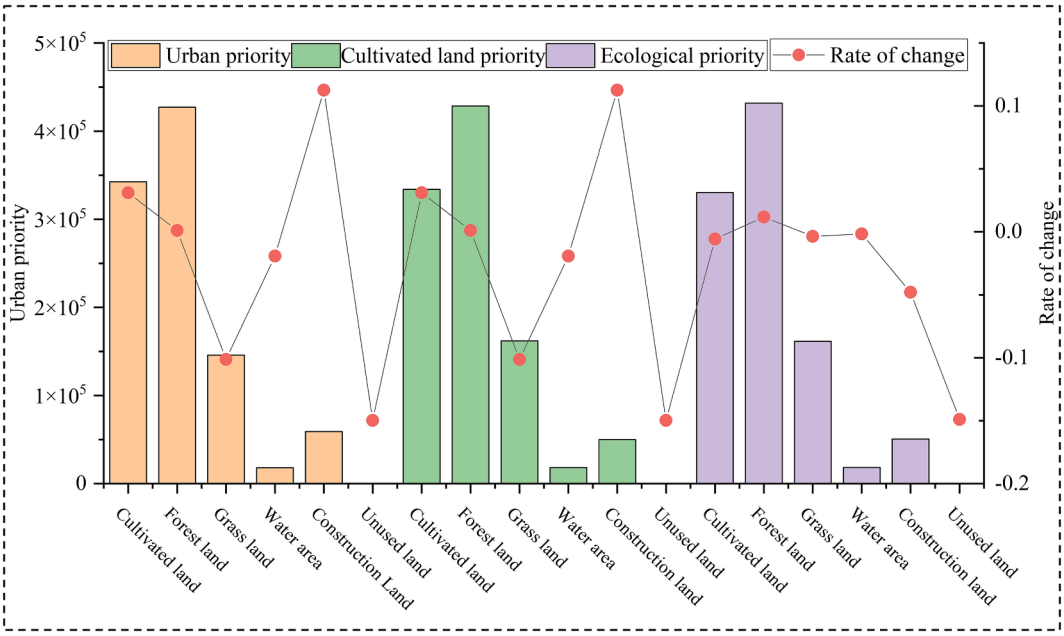

Fig. 8. Comparison of various land use areas under three scenarios.

the area of other land types would decrease. Although the reduction of construction land and unused land was more apparent, the overall change in the region's land types was minimal.

Within the context of ecological priority development, the Sanmenxia Ecological Reserve was considered a restricted change area. The forest area showed a slight increase, while other land types decreased. Overall, changes in all types of land areas were marginal, with characteristics closely aligning with the cultivated land priority development scenario.

The carbon sink of land use in different scenarios was calculated using the carbon density method, based on land use prediction results for the three scenarios. Figs. 9 and 10 show that under the ecological priority development scenario, the forest carbon sink was significantly higher than in the other scenarios. However, the grassland carbon sink was slightly lower than that of the cultivated land priority scenario but notably higher than the urban priority scenario. Under the cultivated land priority scenario, the carbon sequestration of grassland substantially surpassed that of other land uses. For the urban priority development scenario, both cultivated land and construction land demonstrated higher carbon sink values.

The expansion level of different land types varied under three scenarios. By calculating the carbon sink of vegetation and soil, we derived the carbon sink of the study area under each scenario. The predictions indicated the highest carbon sink under the ecological priority scenario, followed by the cultivated land priority, with urban priority having the lowest carbon sink, with carbon sinks measuring 1.077×10^8 t, 1.076×10^8 t, and 1.074×10^8 t, respectively. Fig. 10 presents a normalized comparison of the carbon sink of various land uses under three

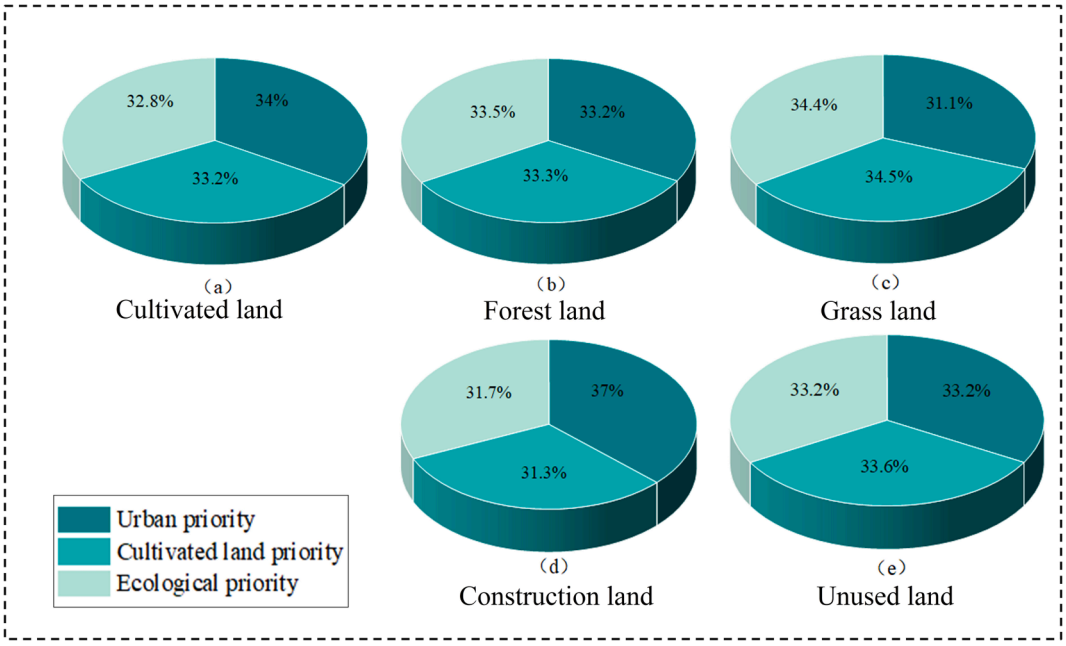

Fig. 9. Comparison of carbon sinks of various land uses under three scenarios.

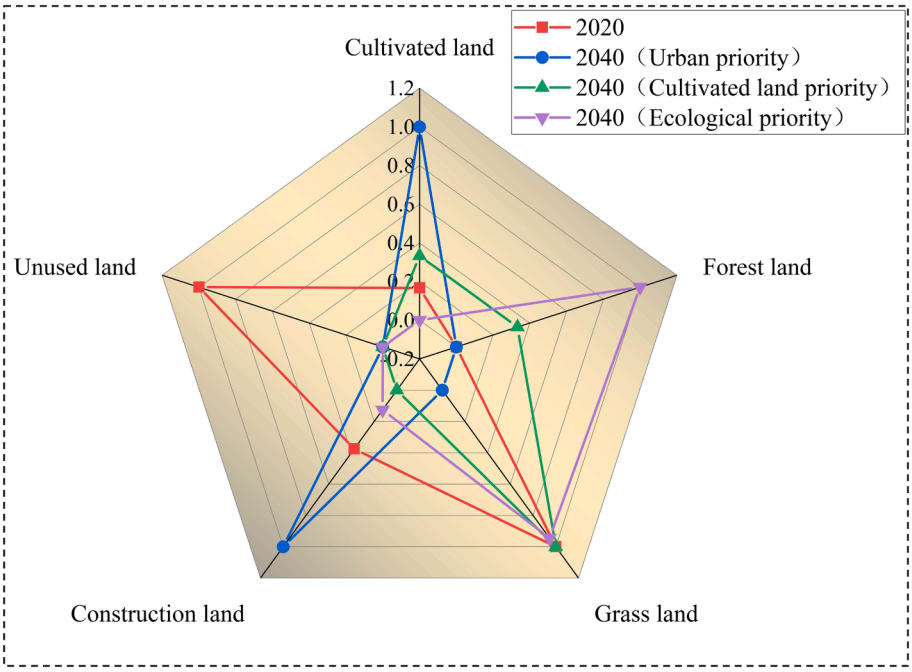

Fig. 10. Comparison of normalized carbon sinks in 2040 under three scenarios.

scenarios. Compared to 2022, the carbon sink of construction land and cultivated land changed more noticeably under the urban priority development scenario. The carbon sink of grassland under the cultivated land priority scenario saw a substantial increase, while under the ecological priority scenario, the carbon sink of forest land and grassland rose significantly.

Fig. 11 presents the average carbon sequestration distribution across three regions, showcasing notable gaps. Using GIS software, we partitioned Sanmenxia's carbon sequestration into various villages and towns, displaying the average distribution of carbon sequestration in Sanmenxia. The carbon sink value was lower in the north and higher in the south. Lushi County constituted a high carbon sink area, Lingbao City represented a medium carbon sink area, while Binhu District, Mianchi County, and Yima City were low carbon sink areas. Shanling Basin and Mianchi Basin were clusters of low carbon sink value, especially under the urban priority development scenario where carbon sink values would decrease as cities and towns expand. The Lushi Basin, bounded by Xiaoshan Mountains, Funiu Mountains, and Xiong'er Mountains, witnessed restrained urban expansion due to its topography. Consequently, even under the urban priority scenario, this region would maintain high carbon sequestration.

Under the cultivated land priority and ecological priority development scenarios, the average carbon sink value among Sanmenxia's towns was relatively small. The average carbon sink value in Shanling Basin and Mianchi Basin was higher than under the urban priority development scenario. The carbon sink in the northern part of the Lushi Basin decreased when compared to the urban priority development scenario. This decrease in average carbon sink is primarily due to the expansion of cultivated land and the decline of grassland in this area, as indicated by the land use change analysis.

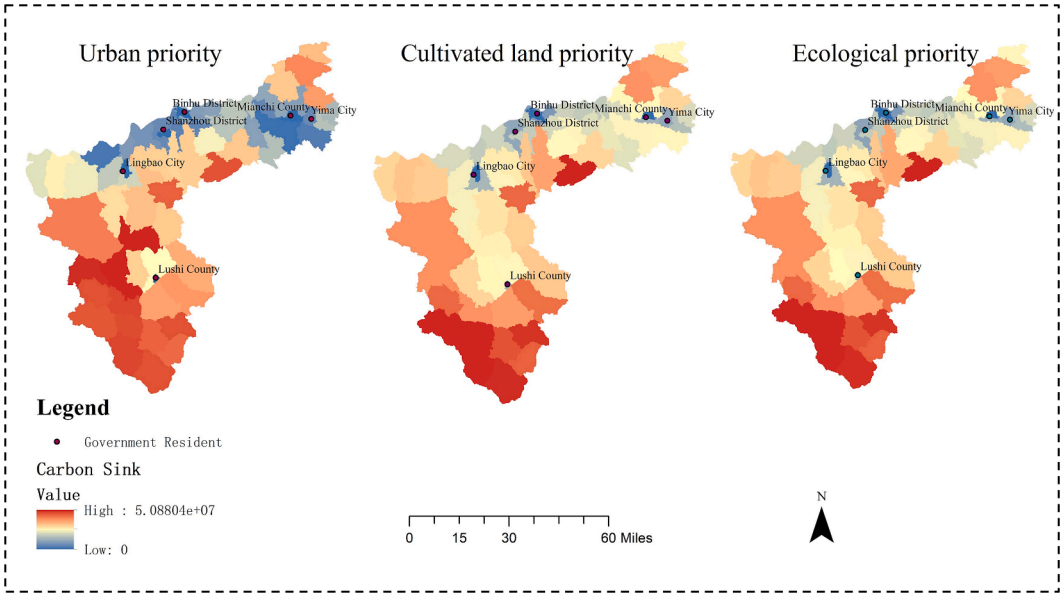

Fig. 11. Distribution of the average carbon sink under three scenarios.

As economic and societal development continues, the regional difference in urban carbon sink mean value continues to grow, leading to a tension between land space development and protection. Under the scenario of protecting cultivated land and maintaining ecological security, the regional mean carbon sink difference would decrease, particularly with improved construction land use efficiency.

5. Discussion

5.1. Spatial carbon sink prediction results

The change of land use pattern plays an important role in regional social, economic and ecological comprehensive benefits, and also affects the carbon storage of terrestrial ecosystem (Liu et al., 2023). Multi-scenario simulation of regional land use change in future years is of great significance for optimizing land use pattern and improving land space carbon sink capacity (Yang et al., 2022).

In our investigation, we predicted land use and carbon sink alterations under three distinct scenarios in Sanmenxia City to explore the evolving trends of the regional carbon sink. Our simulations indicated that the total carbon sink under the urban-centric development scenario would be reduced in 2040 compared to 2020. Conversely, the ecological and agricultural land preservation scenarios are projected to bolster the regional carbon sink value by 2040. This outcome can be attributed to the stipulations in the latter scenarios that prevent the transformation of ecological reserves and prime croplands into alternative land categories. As a result, urban and settlement encroachments on other land types diminished, facilitating the expansion of forests and grasslands and amplifying their ecological service functions.

In addition, relevant studies show that urban carbon sink capacities typically increase as the distance from the city centers increases. Natural land use types such as forest land, grassland and cultivated land and land use types such as scenic areas, nature reserves and important forest areas play the role of urban ecological barriers in the region, so carbon sink per unit area is generally on the rise (Xu et al., 2018). The historical data and predictive outcomes from this study indicate consistent characteristics in the distribution of carbon sink values. Due to the influence of topography and urban development, the low carbon sink areas were mainly concentrated in the dense urban areas such as Shanling Basin and Mianchi Basin, while the high carbon sink areas were mainly concentrated in the mountainous areas in the central and southern part of Sanmenxia City. Among them, Lingbao city, Shanzhou District, Binhu District, Mianchi County, and Yima City had significantly expanded the scale of construction land, showing a state of low carbon sink. Because of the limitation of ecological protection and water area, the scale of urban construction land in Lushi County is small, which leads to the higher average carbon sink value in this area.

5.2. Prediction results of carbon sink development trend

Highlighting the significance of carbon sinks is crucial in determining the best trajectory for regional carbon neutrality (Li et al., 2022). This study's predictive outcomes illuminate the carbon sink evolution under various development scenarios.

The development trend of the carbon sink in Sanmenxia from 2000 to 2040 was charted using a fit of both historical carbon sink data and predicted data from the three scenarios. As demonstrated in Fig. 12, the land use carbon sink in Sanmenxia overall followed a trend of rising, then falling, and finally rising again. Historical data show that the land use carbon sink in the study area peaked in 2005, followed by a consistent decline from 2005 to 2020.

The forecast data indicate that under the urban priority development scenario, the land use carbon sink will continue to decline from 2020 to 2030, with a gradual increase post-2030. However, by 2040, the land use carbon sink will still be lower than that in 2020. Under the cultivated land priority and ecological priority scenarios, restrictions from the cultivated land red line and ecological reserves optimized the land use structure, leading to an increasing carbon sink trend post-2020. As future land development and utilization unfold, green, low-carbon ecological protection must be considered, along with the improvement of land use efficiency and spatial structure optimization in areas with low carbon sinks.

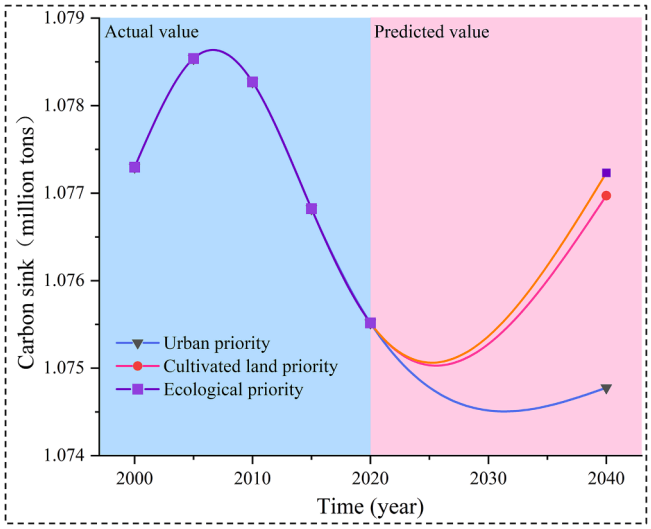

Fig. 12. Development trend of carbon sink under three scenarios.

The "double carbon" strategy sets a 2030 deadline for peak carbon levels. In this plan, the green development action for urban and rural construction aims to enhance the optimization of urban and rural spatial layouts and promote low-carbon transformation of urban and rural construction. The carbon sink enhancement campaign also underscores the need for strengthened land space planning and use control.

Predictions show that the carbon sink under the three development scenarios would continue to decline post-2020, hitting the lowest point around 2030. In the urban priority development scenario, the land use carbon sink is expected to reach a minimum of 107.442 million tons in 2030. This is consistent with the urbanization development scenario set out in the Sanmenxia General Plan for Land Space (2020–2035). The cultivated land priority and ecological priority scenarios would reach their lowest values, 107.501 million tons and 107.508 million tons, respectively, in 2029 and 2028. The timing of these lows is earlier than that of the urban priority scenario. Thus, the results of this study can offer guidance for regional "double carbon" goals and ecological protection.

6. Conclusion and recommendation

Taking Sanmenxia as the research area, this paper explored the influence of land type transformation on carbon sink and predicted the future carbon sink of the region. The main conclusions are as follows:

(1) The historical data showed that the cultivated land, forest land, and construction land in Sanmenxia City showed an overall increasing trend from 2000 to 2020. Among them, cultivated land, forest land, and construction land increased by 3.27 %, 1.01 %, and 24.09 %, respectively. The area of grassland and water decreased by 13.3 % and 1.72 %, respectively. Analyzing the data spatially, the northern basin of the study area underwent pronounced land-use shifts. Urban areas predominantly occupy this region, and the significant expansion of developed land correspondingly reduced the carbon sink capacity. Conversely, the southern segment, characterized by mountainous terrain, witnessed minimal land-use changes, ensuring a consistent carbon sink value.

(2) The FLUS model had a good simulation effect on land use in Sanmenxia City, with a Kappa coefficient of 0.85. According to the simulation of the three scenarios, it was easy to find that the development scenarios of ecological priority and cultivated land priority would be conducive to improving regional carbon sink value by 2040. Specifically, regional cropland, forest, and grassland were preserved due to the ecological red line and the restriction of basic farmland. This would increase the carbon sink value of the study area by 145 thousand tons and 171 thousand tons, respectively, compared with 2020.
(3) Predictions for all three developmental scenarios suggest an initial dip followed by a rise in the study area's carbon sequestration from 2020 to 2040. Under the urban-focused scenario, the carbon sink dipped to its lowest in 2030. For the other scenarios, the trough occurred around 2028, with values higher than the urban-focused approach, and then experienced a notable surge.

Regional carbon sink is a key indicator of an area's ecological health. Changes in land use and land cover have a direct impact on carbon sink in vegetation and soil. In particular, converting forests to cropland leads to the loss of carbon in soil, while allowing cropland to revert to forests increases carbon stocks in soil and biomass (Houghton, 2018). Predictions from this study indicate that scenarios prioritizing ecological and cultivated land conservation are beneficial for regional low-carbon development. Building on prior research, it is evident that the carbon sink abilities of grassland, cultivated land, and forests are influenced by management practices and environmental conditions (Wang et al., 2023b; Wang et al., 2021b). Therefore, in order to achieve the goal of "carbon peak" and "carbon neutrality" in the region, it is necessary to consider cultivated land conservation and ecological protection. Upholding strict ecological boundaries and protecting nature reserves can promote vegetation growth and recovery, potentially reversing environmental degradation trends in some areas. The expansion of construction land was a key factor leading to the decline of carbon sink in the study area. Therefore, consolidating development and minimizing human disturbances are essential for maintaining regional carbon sink. These findings are valuable for guiding future land-use planning with an emphasis on ecological conservation.

This research enhances our comprehension of how shifts in land use impact carbon sink at a municipal level. By forecasting future carbon sink dynamics in the study area, we gauged the implications of land use alterations on regional carbon sink under different development paradigms. These insights offer valuable guidance for regional urban growth strategies, spatial land planning, and ecological conservation endeavors.

7. Statements

7.1. Ethics approval

Consent.

7.2. Consent to participate

Agree to participate.

7.3. Consent for publication

Agreement for publication.

Funding

This research was funded by Key Project of National Natural Science Foundation of China (Grant No. U22A20620) and Key Project of National Natural Science Foundation of China (Grant No. U21A20108).

CRediT authorship contribution statement

Yisha Pan: Writing – original draft. **Hebing Zhang:** Supervision. **Chongyang Wang:** Data curation. **Yongduo Zhou:** Writing – review & editing.

Declaration of Competing Interest

The authors declare that they have no known competing financial interests or personal relationships that could have appeared to influence the work reported in this paper.

Data availability

Data will be made available on request.

References

Alison, R., Brad, R., Girija, P., William, B., 2016. Direct and indirect land-use change as prospective climate change indicators for peri-urban development transitions. J. Environ. Plann. Manage. 59 (4) https://doi.org/10.1080/09640568.2015.1035775.

An, H., Wu, X., Zhang, Y.R., Tang, Z.S., 2019. Effects of land-use change on soil inorganic carbon: A meta-analysis. Geoderma 353, 273–282. https://doi.org/10.1016/j.geoderma.2019.07.008.

Barati, A., Zhoolideh, M., Azadi, H., Lee, J., Scheffran, J., 2022. Interactions of land-use cover and climate change at global level: How to mitigate the environmental risks and warming effects. Ecol. Ind. 146, 109829 https://doi.org/10.1016/j.ecolind.2022.109829.

Díaz-Puente, F., Schmid, T., Pelayo, M., Rodríguez-Rastrero, M., Sierra, H.M., O'Neill, T., López-Martínez, J., 2021. Abiotic factors influencing soil microbial activity in the northern Antarctic Peninsula region. Sci. Total Environ. 750 https://doi.org/10.1016/j.scitotenv.2020.141602.

He Y., Ma J., Zhang C., Yang H. 2023. Spatio-Temporal Evolution and Prediction of Carbon Storage in Guilin Based on FLUS and InVEST Models. *Remote Sensing* (5). https://doi.org/10.3390/RS15051445.

He, Z., Xie, L., Liang, B., Deng, X., Yan, S., Tong, Y., Li, X., 2020. Study on land use simulation based on CA-Markov Model in Lijiang River Basin. Ecolog. Sci. 39 (05), 142–150. https://doi.org/10.14108/j.cnki.1008-8873.2020.05.017.

Houghton, R., 2018. Interactions Between Land-Use Change and Climate-Carbon Cycle. Current Climate Change Reports. 41 (2), 115–127. https://doi.org/10.1007/s40641-018-0099-9.

Huang, Y., Chen, T., Hu, D., Lin, T., Zhu, W., Zhang, G., Xue, X., 2023. Spatiotemporal patterns and influencing factors of urban ecological space availability in coastal cities of China during rapid urbanization. Ecol. Ind. 154, 110757 https://doi.org/10.1016/j.ecolind.2023.110757.

Josephine, M., 2023. Environmental integrity of forest offsets in a changing climate: embedding future climate in Australia's sinks policy regime. J. Environ. Plan. Manag. https://doi.org/10.1080/09640568.2023.2167196.

Letourneau, A., Verburg, P., Stehfest, E., 2012. A land-use systems approach to represent land-use dynamics at continental and global scales. Environ. Model. Softw. 33, 61–79. https://doi.org/10.1016/j.envsoft.2012.01.007.

Li, Q., Li, J., Jiang, Z., Bian, J., 2020. System degradation modeling with individual differences and maintenance decision based on semi-Markov process. Comput. Integr. Manuf. Syst. 26 (2), 331–339. https://doi.org/10.13196/j.cims.2020.02.006.

Li, Z., Xue, W., Winijkul, E., Shrestha, S., 2023. Spatio-Temporal Dynamics of Non-Point Source Pollution in Jiulong River Basin (China) Using the Soil & Water Assessment Tool Model in Combination with the GeoSOS-FLUS Model. Water. 151 (15), 2763. https://doi.org/10.3390/w15152763.

Li, W., Zhang, S.H., Lu, C., 2022. Exploration of China's net CO_2 emissions evolutionary pathways by 2060 in the context of carbon neutrality. Sci. Total Environ. 831, 154909 https://doi.org/10.1016/j.scitotenv.2022.154909.

Lin, G., Jiang, D., Fu, J., Chao, C., Zhang, D., 2021. Spatial conflict of production-living-ecological space and sustainable-development scenario in Yangtze River Delta agglomerations. Sustainability 12 (6), 1175. https://doi.org/10.3390/su12062175.

Liu, X., Liang, X., Li, X., Xu, X., Ou, J., Wang, S., Pei, F., 2017. A future land use simulation model (FLUS) for simulating multiple land use scenarios by coupling human and natural effects. Landsc. Urban Plan. 168, 94–116. https://doi.org/10.1016/j.landurbplan.2017.09.019.

Liu, J., Wang, Z., Duan, Y., Li, X., Zhang, M., Liu, H., Xue, P., Gong, H., Wang, X., Chen, Y., 2023. Effects of land use patterns on the interannual variations of carbon sinks of terrestrial ecosystems in China. Ecol. Ind. 146V https://doi.org/10.1016/j.ecolind.2023.109914.

Ma, X., Wang, Z., 2015. Research progress on the impact of land use change on regional carbon sources and sinks. Acta Ecol. Sin. 35 (17), 5898–5907. https://doi.org/10.5846/stxb201312112932.

Michael, A., Evans, D., Barry, H., Sofie, S., 2020. Biomass and carbon stocks of organic and conventional cocoa agroforests, Ghana. Agr Ecosyst Environ 306. https://doi.org/10.1016/j.agee.2020.107192.

Nel, L., Boeni, A., Prohaszka, V., Szilagyi, A., Kovacs, E., Pasztor, L., Centeri, C., 2022. InVEST Soil Carbon Stock Modelling of Agricultural Landscapes as an Ecosystem. Sustainability. 14 (16) https://doi.org/10.3390/su14169808.

Rao, Y., Zhang, J., Wang, K., Jepsen, M., 2021. Understanding land use volatility and agglomeration in northern Southeast Asia. J. Environ. Manage. 278 (1), 111536 https://doi.org/10.1016/j.jenvman.2020.111536.

Rhys, W., Corin, J., Davide, G., Simon, S., 2021. Decarbonising steel production using CO2 Capture and Storage (CCS): Results of focus group discussions in a Welsh steel-making community. Int. J. Greenhouse Gas Control 104. https://doi.org/10.1016/j.ijggc.2020.103218.

Robinson, T., Di Vittorio, A., Alexander, P., Arneth, A., Barton, M., Brown, D., Kettner, A., Lemmen, C., O'Neill, B., Janssen, M., Pugh, T., Rounsevell, M., Rabin, S., Syvitski, J., Ullah, I., Verburg, P., 2018. Modelling feedbacks between human and natural processes in the land system. Earth Syst. Dyn. 9 (2), 895–914. https://doi.org/10.5194/esd-9-895-2018.

Wang, T., Gong, Z., Deng, Y., 2021a. Identification of priority areas for improving quality and efficiency of vegetation carbon sink in Shaanxi province based on land use change. J. Nat. Resour. 37 (05), 1214–1232. https://doi.org/10.31497/zrzyxb.20220508.

Wang, M., Hu, Z., Wang, X., Li, X., Wang, Y., Liu, H., Han, C., Cai, J., Zhao, W., 2023a. Spatio-Temporal Variation of Carbon Sources and Sinks in the Loess Plateau under Different Climatic Conditions and Land Use Types. Forests 14 (8), 1640. https://doi.org/10.3390/f14081640.

Wang, X., Ma, B., Li, D., Chen, K., Yao, H., 2020. Multi-scenario simulation and prediction of ecological space in Hubei Province based on FLUS model. J. Nat. Resour. 35 (01), 230–242. https://doi.org/10.31497/zrzyxb.20200119.

Wang, Z., Xu, L., Shi, Y., Ma, Q., Wu, Y., Lu, Z., Mao, L., Pang, E., Zhang, Q., 2021b. Impact of Land Use Change on Vegetation Carbon Storage During Rapid Urbanization: A Case Study of Hangzhou, China. Chinese Geograph. Sci. 31 (2), 209–222. https://doi.org/10.1007/s11769-021-1183-y.

Wang, Z., Lin, L., Zhang, B., Xu, H., Xue, J., Fu, Y., Zeng, Y., Li, F., 2023b. Sustainable urban development based on an adaptive cycle model: A coupled social and ecological land use development model. Ecol. Ind. 154, 110666 https://doi.org/10.1016/j.ecolind.2023.110666.

Xu, Q., Dong, Y., Yang, R., 2018. Influence of the geographic proximity of city features on the spatial variation of urban carbon sinks: A case study on the Pearl River Delta. Environ. Pollut. 243, 354–363. https://doi.org/10.1016/j.envpol.2018.08.083.

Xu, X., Wang, S., Rong, W., 2023.Construction. of ecological network in Suzhou based on the PLUS and MSPA models. Ecol. Ind. 154 (110740) https://doi.org/10.1016/j.ecolind.2023.110740.

Yang, B., Bai, Z., Zhang, X., 2017. Research on carbon emission from land damage in extra large open-pit coal mine: a case study of Pingshuo mining area. China Land Sci. 31 (6), 59–69.

Yang, W., Min, Z., Yang, M., Yan, J., 2022. Exploration of the Implementation of Carbon Neutralization in the Field of Natural Resources under the Background of Sustainable Development-An Overview. Int. J. Environ. Res. Public Health 19 (21), 14109. https://doi.org/10.3390/ijerph192114109.

Yi, D., Ou, M., Guo, J., Han, Y., Yi, J., Ding, G., Wu, W., 2022. Research progress and trend prospect of carbon emission and low-carbon optimization of land use. Resour. Sci. 44 (08), 1545–1559. https://doi.org/10.18402/resci.2022.08.02.

Yu, Q., Wu, Z., Wang, Y., 2023. A simulation model of land use change coupled with evolutionary Algorithm and FLUS model. J. Geoinformation Sci. 25 (03), 510–528. https://doi.org/10.12082/dqxxkx.2023.220637.

Zhang, M., Lai, L., Huang, X., Chuai, X., Tan, J., 2013. The carbon emission intensity of land use conversion in different regions of China. Resources Science 35 (04), 792–799 https://doi.org/CNKI:SUN:ZRZY.0.2013-04-016.

Zhang, X., Zhang, X., Li, D., Lu, L., Yu, H., 2021. Multi-scenario simulation of the impacts of urban land use change on ecosystem service value: A case study of Shenzhen City. Acta Ecol. Sin. 42 (06), 2086–2097. https://doi.org/10.5846/stxb202102270546.

Zhao, J., Shao, Z., Xia, C., Fang, K., Chen, R., Zhou, J., 2023. Ecosystem services assessment based on land use simulation: A case study in the Heihe River Basin, China. Ecological Indicators. 143, 109402 https://doi.org/10.1016/j.ecolind.2022.109402.

Zhu, S., Shu, B., Ma, X., Liang, X., Yao, Q., 2017. Delimitation of urban land growth boundary based on "inverse planning" concept and FLUS model: A case study of Jiawan District, Xuzhou City. Geography Geo-Inform. Sci. 33 (5), 80–86. https://doi.org/10.3969/j.issn.1672-0504.2017.05.013.